Centralized-Decentralized Control of Responsive Demand to Enable Primary and 10-min Reserves

CCTC 2015 Paper Number 1570042893

M. Chakir[1], I. Kamwa[2], Fellow, IEEE , H. Le Huy[1], Senior Member, IEEE

[1] Laval University, Québec, Canada
[2] Research Institute of Hydro-Québec, Varennes, Québec, Canada

Abstract

Abstract—High penetration of renewable energy, bringing generation closer to consumption and splitting power systems into micro grids after disturbances are trends and actions of future power systems. Providing ancillary services will therefore be a challenging task due to the lack of conventional spinning reserves and storage devices. Demand response is an attractive way to provide ancillary services for smart grid due to its two-way communication and customer contribution to the control of the grid. This paper presents a centralized-decentralized control of responsive demand to primary and 10-min reserves. Two control techniques are applied to each control mode: a multi-band power system stabilizer and a droop control (DC). The effectiveness of these control strategies is demonstrated on a modified IEEE 14-bus system connected to a 14-bus distribution system operating at 100% capacity and subjected to a severe generation loss.

Keywords: Demand response (DR), Multi-Band power system stabilizer, Micro-grids, Droop control (DC

Résumé

1. Introduction

INTRODUCTION

To ensure reliable operation of the power system, the balance between power generation and demand must be kept in normal operation, after normal load and generation variations or after a major disturbance such as a large generation loss, loss of an interconnection or other unforeseen events that could lead to collapse of the grid. The contingency response to such events is historically obtained from the generation side by correcting the mechanical power of the generators using primary control and area generation control [1,4]. Likewise, dynamic stability is strengthened by regulating the generators' excitation voltage through power system stabilizers, and more recently, transmission level FACTS devices [1,4]. The demand side is used just for extreme cases in the form of load shedding.

The smart grid trend to include intermittent renewable power generation (wind power, photovoltaic cells, etc.) such as distributed resources is leading utilities to install more spinning and non-spinning reserves to compensate for the fitfulness of generated power, thereby increasing costs but creating more pollution associated with conventional power plants. This is inconsistent with the philosophy of the smart grid that seeks to reduce both the energy cost and pollution. To deal with this paradox, conventional solutions are to be replaced by alternatives that meet the objectives of the smart grid.

Demand response (DR) has always been a very interesting way to obtain power system ancillary services [8] but it was hampered by a poor communication network and inadequate information and computer technologies. During the last decade, advances in communication and information technologies have boosted many studies and projects to test and apply DR and load control to power system ancillary services, including load as a resource for ancillary services, interruptible load and dynamic pricing [6-10, 37-39]. This evolution in DR makes it a very interesting solution to replace conventional spinning and non-spinning reserves because it could enable the same facilities with a faster response, lower cost, good dispersion in the distribution system and less pollution [12,33,34]. The Federal Energy Regulatory Commission (FERC) mentioned in its assessment report on the DR potential in the United States that the peak demand annual growth rate is about 1.7%, reaching 950 GW by the year 2019 and, according to the type of DR applied (dynamic pricing, direct load control, interruptible tariffs, autonomous response control (ARC) or DR operated by Independent System Operators (ISO)), up to 20% (188 GW) of the peak demand could be alleviated [32].

Some authors [3] classified these types of DR in two control categories: a centralized one, in which we find DLC, and a decentralized one which contains ARC. All types of DR control are applicable to medium and large industrial and commercial loads but only dynamic pricing, DLC and ARC could be available for domestic appliances. In the DLC, the power consumption of loads is directly controlled through smart meters by a central controller. In this demand response type, frequency is usually considered as the center of inertia (COI) frequency of the power system and is controlled by one central controller. On the other hand, in ARC, frequency is measured locally or near to controllable loads enabling control of each load or small aggregations of loads by local controllers.

Therefore, to achieve these two types of DR, available controllable loads with significant presence in the power system are needed. Residential electric water heaters (EWHs) equipped with a hot-water storage tank have an electricity consumption of about 11% of the total electricity consumption and the figure increases to over 30% during peak demand hours [20,25]. In addition, using such loads for the short durations required to enable spinning reserves would have no impact on customer comfort [17],[35]. They are therefore motivating loads for responsive demand control due to their availability and their natural response capabilities that match the response speed, duration and frequency needed to support spinning and non-spinning reserves [41].

Several studies of DR have been made recently for diverse purposes. The cost-effectiveness analysis of DR in the power market and the development of plans to realize such benefits are reported in [6-10], [21,28]. The capability of loads to provide reserves for control frequency has been widely studied [14]-[17], [20]. Authors in [30-33] studied DR to improve power system stability. Studies on the effectiveness of centralized and decentralized control of DR to enable reserves are limited and they didn’t focus on performing realistic simulations based on accurate power system models [18,19,22,23,25-29].

This paper presents a centralized and a decentralized control of responsive demand at both the transmission and the distribution levels to allow spinning and 10-min reserves, applied to a modified standard IEEE 14-bus network connected to the CIGRÉ North-American medium-voltage benchmark system.

The two control schemes are modeled and simulated in Matlab/Simulink SimPowerSystem (SPS). Their effectiveness is demonstrated by simulating the four following simulations. 1) Centralized control with MB-PSS and no reserves, 2) Centralized control with DC and no reserves, 3) Decentralized control with MB-PSS and no reserves and 4) Decentralized control with DC and no reserves ('No reserves' implies that our system operates at 100% of its generating capacity). Their performances are thoroughly analyzed and compared. Each control mode is implemented using two different controllers: a multi-band power system stabilizer (MB-PSS) and a droop controller (DC)".

2. Centralized-Decentralized control

The role of controls in a power system is to keep system variables within their limits. Frequency is a key variable of the power system and is responsive to load or generation variations. DLC is a frequency control that acts on loads to maintain frequency at acceptable levels. It can be centralized or decentralized depending on where and how frequency is measured and controlled. In centralized mode, there is just one frequency measurement controlled by single controller, while in the decentralized mode, frequency is measured at different strategic points of the grid, generally near the controllable loads.

In the case of EHWs as loads, the difference between the two modes is also seen in the action of the controllers. In the centralized mode, depending on the power system event, the controller signal is used to connect or disconnect loads via a communication device (e.g. a smart meter). In decentralized mode, on the other hand, the controller signals are continuously modifying the power consumption of each load via power electronic devices (e.g. triacs).

2.1. Centralized mode

As mentioned above, in centralized mode, the frequency of the overall system is controlled by one controller which is represented by the center of inertia (COI) frequency of the power system. In this paper, a simple method is used to estimate COI, which is represented as the average of the generator frequencies. Figure 1(a) presents a diagram that explains the operating principle of the centralized mode.

The frequency is calculated using the rotor speed of the generators. The central controller is a MB-PSS or a DC. The controller input is the COI rotor speed deviation ($d\omega$) when a MB-PSS is used, whereas it is the COI frequency (Hz) when a DC is used as the controller. Outputs of both controllers are dispatched to controllable loads to switch them "on" or "off" via smart meter-Zigbee systems.

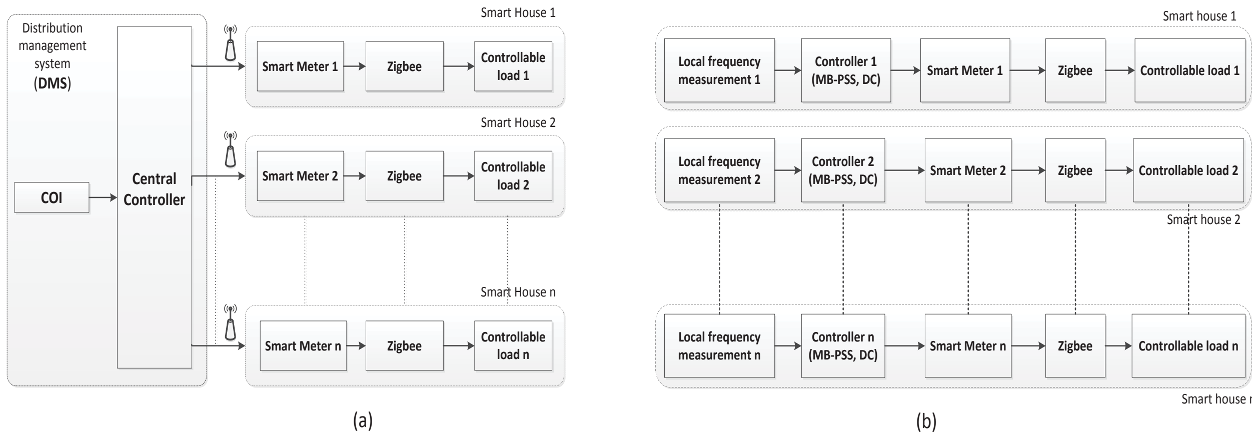

Figure 1. Overview diagram of centralized mode (a) and decentralized mode (b)

2.2. Decentralized mode

In decentralized mode, the frequency is controlled locally or very near to controllable loads. Loads are controlled through power electronic devices to enable a continuous variation of power consumption, then a smoother demand response. Figure 1(b) shows an overview of the decentralized mode.

One of the benefits of this mode is that it can allow low-power operation of controllable loads even in a frequency droop, whereas the centralized control switches off the same load. This could be very important for ensuring particular clients' comfort when the controllable loads are EWHs or air-conditioning.

The frequency is measured from the positive-sequence voltage at buses near controllable loads. The number of measurements taken equals the number of controllable loads. Loads are controlled individually and are dependent only on their frequencies at their respective location. This could be of great benefit in cases of islanding because it keeps the demand response control in islands and in the main grid, contrary to the centralized mode where we lose control in islands.

To minimize control devices in the decentralized mode, loads in the same areas could be aggregated to form small groups, each controlled by one controller.

3. Modified IEEE 14-bus system

This section describes the modified IEEE 14-bus system model. It is composed of a 345-kV transmission system and a 12.47-kV distribution system. The system model is a Phasor representation. It has been realized in Matlab\Simulink SPS.

The network is a 345-kV network comprising three synchronous generators with a hydraulic turbine and governor systems (GSs), three synchronous compensators (SCs), eight transformers, 19 transmission lines, 15 breakers and 11 loads. Each generator has a governor and an excitation system to control speed and voltage. Table 1 shows the generator data.

Figure 2. shows the modified IEEE 14-bus system.

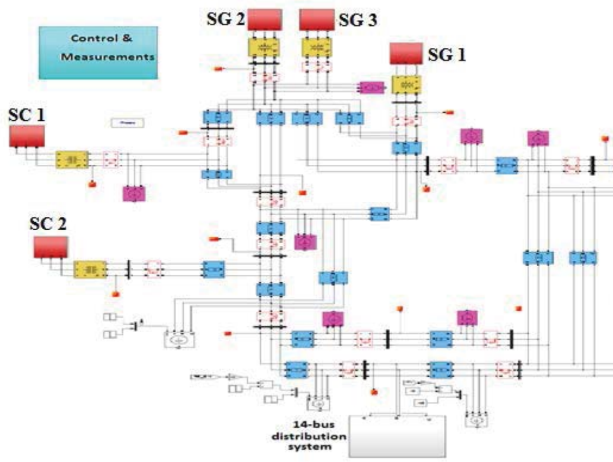

Figure 2. Modified IEEE 14-bus system

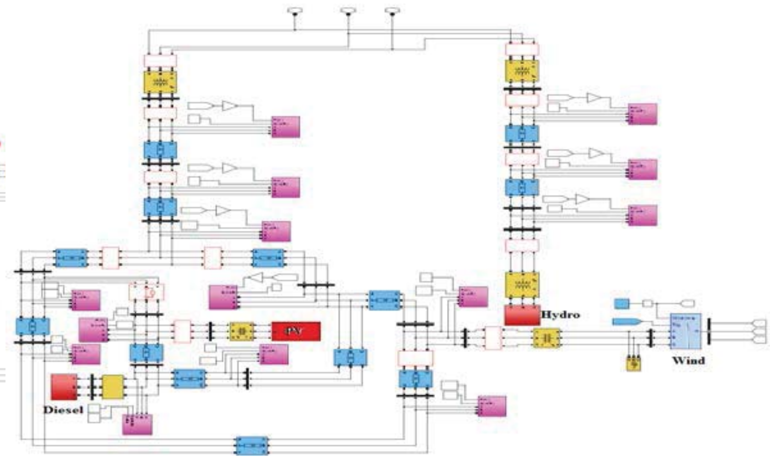

Figure 3. 14-bus distribution system

Breakers serve to simulate the protection actions and enable islanding scenarios. Complete line, transformer and other system component data is available in [43].

Table 1: Data of generators and SC (Red boxes in Figure 2.)

Generators	Data
SG 1 (Hydraulic turbine)	300 MVA, 13.8 kV, 60 Hz
SG 2 (Hydraulic turbine)	50 MVA, 13.8 kV, 60 Hz
SG 3 (Hydraulic turbine)	10 MVA, 13.8 kV,60 Hz
SC1(Synchronous compensator)	60 MVA, 13.8 kV, 60 Hz
SC2, SC3	25 MVA, 13.8 kV, 60 Hz

The distribution system is derived from an actual medium-voltage (MV) distribution system, the CIGRÉ North American MV benchmark system. It comprises four distributed generators (DGs), six transformers, eight breakers and a load on each bus. Breakers 1 to 8 are there to allow the simulation of different islanding topologies. DG1 is a 10-MW synchronous generator with a hydraulic turbine and governor system connected to bus B14, DG2 is a 2-MW wind farm connected to bus B7, DG3 is a 5-MW diesel generator connected to bus B9 and DG4 is a 160-kW photovoltaic plant connected to bus B11. Table II summarizes the data of these DGs.

Table II: Data of distributed generators (Red boxes in Figure 3.)

Generators	Data
Grid	5000 MW, 115kV, 60Hz
DG1 (Hydraulic turbine)	10MW, 13kV, 60Hz
DG2 (Wind farm)	2MW, 575V,60Hz
DG3 (Diesel generator)	5MW, 2.4kV, 60Hz
DG4 (Photovoltaic plant)	160kW, 440 V, 60Hz, 30*35 MSX-60 modules,

The complete data for lines, loads and transformers of the network are given in [43]. The PV and wind generator power electronics are represented with phasor models to enable long periods of simulation.

3.1. Loads modelling

Load models are divided into two categories: controllable and non-controllable. Controllable loads are modeled as three-phase dynamic loads whose active power P and reactive power Q vary as functions of the positive-sequence voltage [42]. The load impedance is kept constant if the terminal voltage V of the load is lower than a specified value Vmin. When the terminal voltage is greater than Vmin, the active and reactive powers P and Q of the load vary as follows:

$$P(s) = P_0\,(V/V_0)^{n}{}_{p} *(1+T_{p1}s)/(\ *(1+T_{p2}s)) \quad (1)$$

$$Q(s) = Q_0\,(V/V_0)^{n}{}_{q} *(1+T_{q1}s)/(\ *(1+T_{q2}s)) \quad (2)$$

where V0 is the initial positive-sequence voltage, P0 and Q0 are the initial active and reactive powers at the initial voltage V0, V is the positive-sequence voltage, np and nq are exponents (usually between 1 and 3) controlling the nature of the load, Tp1 and Tp2 are time constants controlling the dynamics of the active power P, Tq1 and Tq2 are time constants controlling the dynamics of the reactive power Q, and np and nq are respectively set at 1.3 and 2 to fit Hydro-Québec load models.

EWHs are perceived as constant power loads. They are represented in our IEEE 14 buses by elements named controllable loads. They are designed to have values from zero (disconnected) to nominal.

The model comprises two constant power dynamic loads. The first one sets the whole load to an initial value Pi. The second receives the active-power value from the controller; it could have a positive or a negative value to increase or decrease the initial consumption depending on the nature of the disturbance. In the event that we have to increase the consumption of the EWHs, heating elements are added to enable higher consumption. In this case, EWHs are perceived as storage devices [20]. Figure 4 shows the implemented load model in SPS.

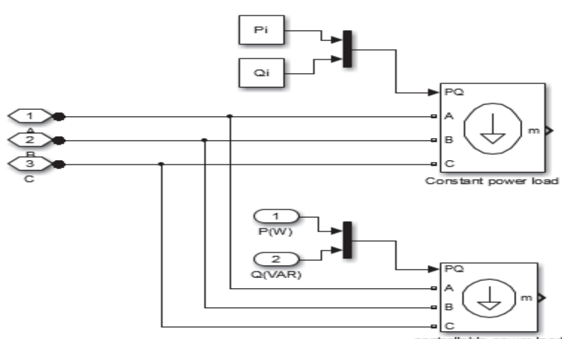

Figure 4. Controllable load model

3.2. Controllers

Two controllers are used: a MB-PSS and a DC. The first is represented by the IEEE Std.421.5 PSS 4B type model [40], with built-in speed transducers whose parameters are fixed according to the manufacturer's specifications. It is based on multiple working bands, as shown in Figure 5.

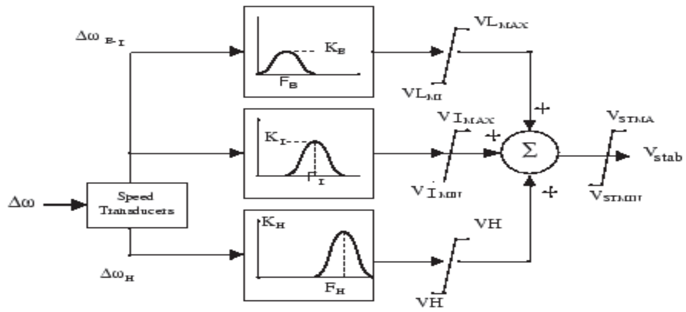

Figure 5. Conceptual representation of MB-PSS

Three separate bands are used, dedicated respectively to the low-, intermediate-, and high-frequency modes of oscillations: the low band is typically associated with the power system global mode, the intermediate with the inter-area modes, and the high with the local modes. Each of the three bands is made of a differential band-pass filter, a gain, and a limiter. The outputs of the three bands are summed and passed through a final limiter producing the MB-PSS output, Vstab. This signal then is dispatched on controllable loads to modulate their active power set point. Figure 6 shows the frequency response of the MB-PSS. It is tuned to maintain our 14-bus system stability by damping power swings after disturbances. Low-frequency (LF) and intermediate-frequency (IF) band filters gains are set respectively to 360 at a center frequency of 1 mHz and 240 at a center frequency of 0.12 Hz, while the high-frequency band filter is switched off by setting its gain to zero. These values were chosen after trial-and-error simulations. The second controller (DC) has the same goal, namely to damp power swings. The control signal sets the instantaneous active power of controllable loads to:

$$P=P_0+\Delta f*P_n \quad (3)$$

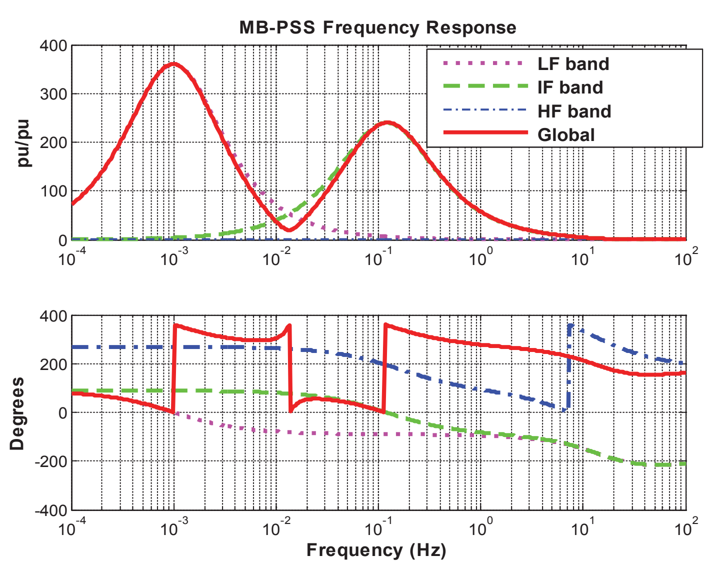

Figure 6. MB-PSS frequency response

With P = instantaneous active power of controllable load; P0 = initial power of controllable load; Δf = difference between reference frequency and measured frequency; and Pn = nominal power of controllable load. In decentralized mode, the frequency measurement is obtained from a derivative of the phase variation of controllable load voltage.

4. Simulations and results

This section presents and discusses the results of the five following simulations: 1)no control, no reserves; 2) no control with reserves;3) centralized control with MB-PSS and no reserves; 4) centralized control with DC and no reserves; 5)decentralized control with MB-PSS and no reserves; and 5) decentralized control with DC and no reserves. The IEEE 14-bus system has a total load of 292 MW and a total production capacity of 372MW, so a spinning reserve of 80 MW is present in generator SG 1 in Figure 2. Controllable loads present a total consumption of 29 MW (10% of the total load): 22 MW on the transmission network and 7 MW on the distribution network. In the last four simulations (controls with no reserves), we removed the 80 MW of reserves with the result that the total production capacity equal to the total load. This means that the IEEE 14-bus system was operating at 100% of its generation capacity. In other words, with no control, any generation loss will cause the whole system to collapse, as seen in the first simulation in Figure 7 (left). This demonstrates the effectiveness of our controls on a power system without reserves. The system is simulated for 700 s. At time t = 5 s, we lost a 10-MW generating unit of (3.4% of total production) switching off generator SG2. This makes it possible to display the behavior of the system in the next 10 min.

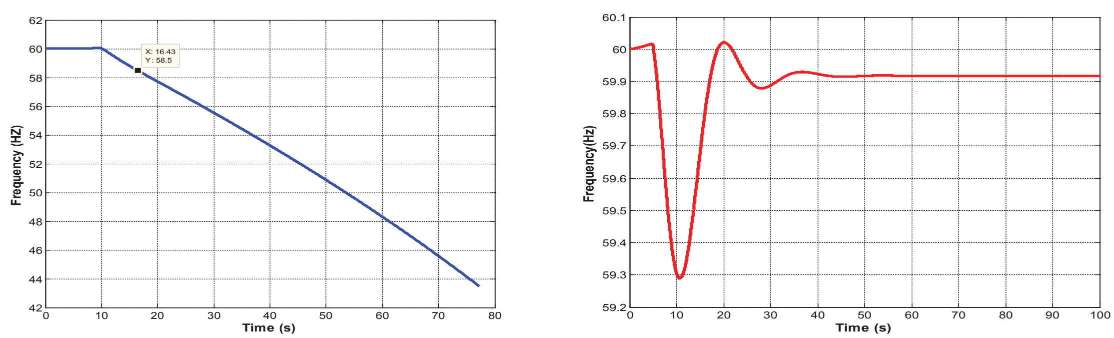

Figure 7: System frequency with no control and no reserve (left) and with 80 MW of spinning reserves and no control (right)

With no reserves, the frequency drops to 58.5 Hz in 6.5 s and continues to fall rapidly; it drops further down to 57 Hz. The second simulation shows the action of reserves after the same generation loss. Figure 7 (right) presents a frequency profile of the same system with no control, but with 80 MW of spinning reserves. Only the first 100 s of simulation is presented in this figure because the system reaches the steady state about 50 s after the fault. After the loss of 10 MW of generation, the frequency drops to 59.3 Hz, and then reaches the steady state of 59.92 Hz after an overshooting of 0.1 Hz. The static error in steady state is caused by the 5% droop control of the generating units. All variables in Figures 8 to 12 are presented in two time ranges in an aim to emphasize their transients and 10-min values.

4.1. Centralized control

This section presents the performances of the centralized control with MB-PSS and DC. The communication delay is represented by à pure delay of 0.25 s. Figure 8 shows the frequencies of the system with controllers compared to the frequency of the system with reserves.

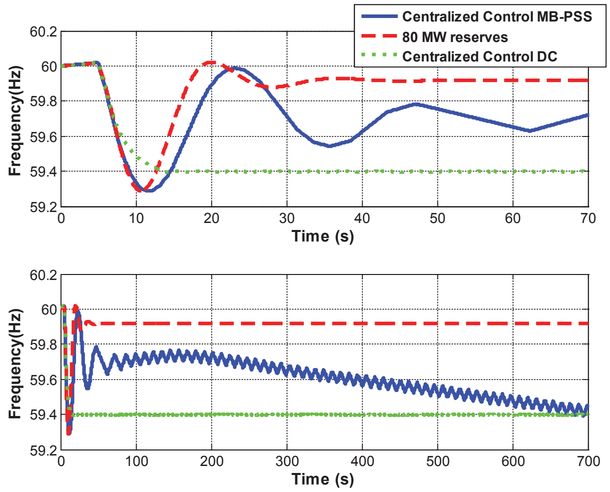

Figure 8. System frequency of centralized control with no reserve/80 MW spinning reserves

After the generation loss, the system with the MB-PSS controller frequency drops to the same level (59.3 Hz) as the system with 80 MW spinning reserves. It then rises to reach 60 Hz and decreases gradually by 0.05 Hz/100 s during the next 10 min to reach 59.4 Hz at 690 s (11.5 min) after the fault. Meanwhile, the system with the DC controller frequency has a different profile compared to the system frequency with spinning reserves and the system with MB-PSS: the post-fault frequency decreases by about 0.13 Hz/s during the first 5 s then reaches a steady state of 59.4 Hz after 7 s. The jitter observed in the frequency profile is caused by the fact that the controllable loads are switched on or off and not controlled linearly. Figures 9 and 10 show the controller outputs and the modulated power after the generation loss. As expected, controllers correct the frequency drop by sending negative signals to controllable loads to switch them off. The MB-PSS output reaches its minimum (-1) after 10 s. Thus, all controllable loads (29.2 MW) are switched off. The MB-PSS output then tends to stabilize at (-0.6) to switch off near about 60% of controllable loads. On the other hand, the DC output steadies at (-0.6) after 12 s and stays at this value for the next 10 minutes.

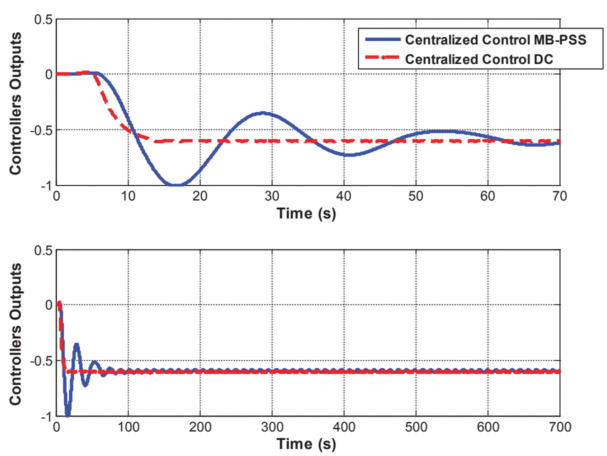

Figure 9. Controllers outputs with centralized control and no reserve/80 MW spinning reserves

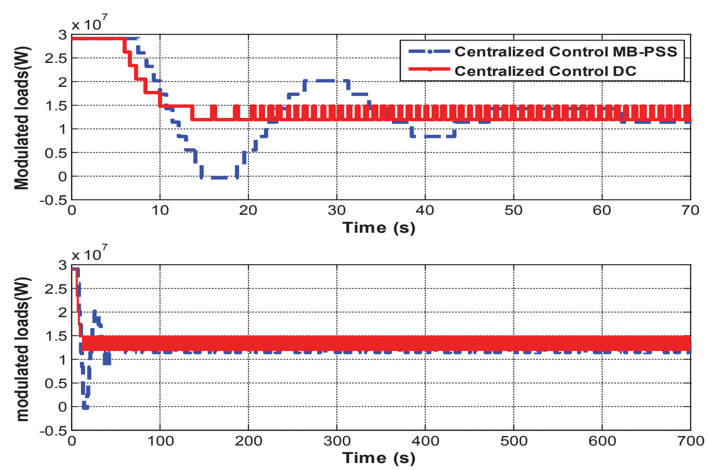

Figure 10. Modulated MW with centralized control and no reserve/80 MW spinning reserves

4.2. Decentralized Control

Figure 11 shows the system frequency with decentralized control. It has the same profile as the frequency with centralized control, although after a fault, the system frequency with decentralized MB-PSS controllers drops to 59.45 (0.15 less than MB-PSS in centralized control) and stays above 59.65 Hz after 10 min while it reaches 59.4 Hz in the centralized mode. Decentralized DC controllers also give better performances in steady state than DC in centralized mode; after the fault, the frequency stays at 59.65 Hz after an overshoot of 0.1 Hz.

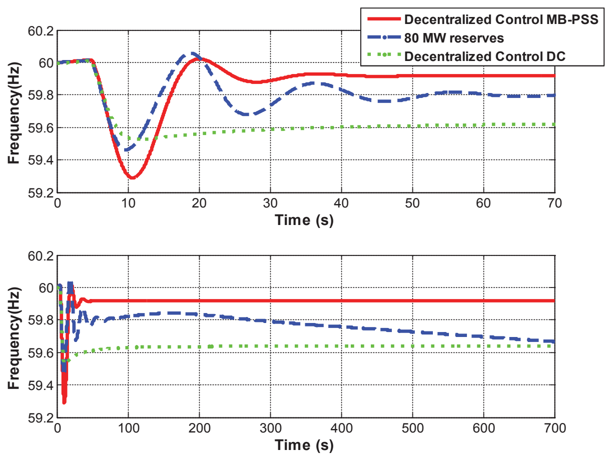

Figure 11: System frequency with decentralized control and no reserve/80 MW spinning reserves

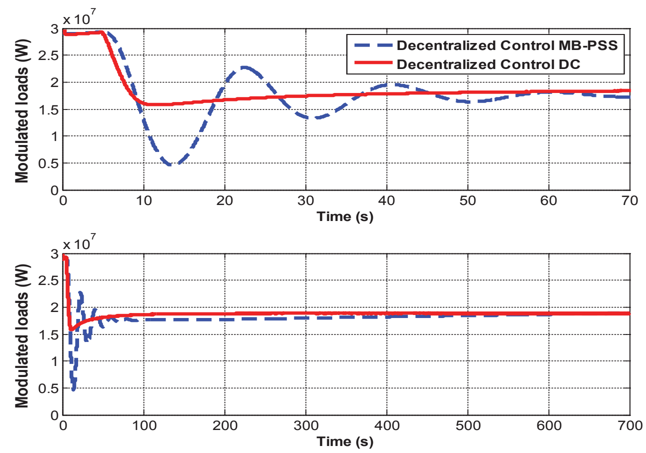

Figure 12. Modulated MW with decentralized control and no reserve/80 MW spinning reserves

Figure 12 shows modulated loads with decentralized control after the generation loss. It should be recalled that in this mode loads are not switched off or on as is the case with centralized control. They are controlled using a dimmer, with the result that their consumption varies continuously depending on the controller signal. For the same event (loss of 10-MW generating unit), decentralized control uses about 6.25 MW (21.4% of controllable loads) less than centralized control, enabling more loads for other unforeseen events. Table 3 shows the performances summary of both control modes. The decentralized mode presents better performances; 21.4% less MW used, a lower frequency dip (0.15 Hz) and keep frequency closer by 0.25 Hz to 60 Hz after 10 min of 10 MW generation loss. We observe that the frequency profile of the decentralized mode do not present the jitter seen in the centralized mode. This is because that loads in this mode are controlled linearly with power electronic device and not switched off or on as in the case of centralized mode.

Table 3: Performances summary of the two control mode

Control Mode	Centralized Control		Decentralized Control		80 MW reserves
Performances	MB-PSS	DC	MB-PSS	DC	
Frequency dip (Hz)	59.3	59.4	59.45	59.55	59.3

Frequency After 10 min of generation loss (Hz)	59.4	59.4	59.65	59.65	59.9
Overshoot (Hz)	0	0	0.05	0	0.01
Controllable Loads used for Control (MW)	17.25	17.25	11	11	–

5. Conclusions

The paper has presented two control modes of a responsive demand to enable primary and 10-min reserves of a modified IEEE 14-bus power system connected to CIGRE's MV benchmark system. The effectiveness of both control modes is demonstrated by phasor simulation of the system in SPS. Both centralized and decentralized controls keep the system frequency at a satisfactory level after a 3.4% loss of total generation. However, decentralized control yields better results than its centralized counterpart by keeping the frequency at a higher level with less controllable loads.

This technology presents the benefit of using a large range of controllable loads (kW for residential EWH to MW for industrial EWH) to accomplish the frequency control. Since the centralized mode controls loads by switching them on or off, using it for large loads will lead to high jitter in the frequency signal that could lead to instable operation. The implementation of this technology needs the installation of smart meters and sophisticated communication network to assure its operation. This paper shows that demand response could substitute efficiently spinning reserves.

6. References

[1] P. Kundur, "power System Stability and Contol," McGraw Hill, Inc., New York, 1994

[2] Fred C. Schweppe, Richard D. Tabores, James L. Kirtley, Hugh R. Outhred, Federick H. Pickle, and Alan J. Cox "Homeostatic Utility Control," *IEEE Transactions on Power Apparatus and Systems*, vol. PAS-99, no. 3, May/June 1980.

[3] Shuai Lu, Nader Samaan, Ruisheng Diao, Marcelo Elizondo, Chunlian Jin, Ebony Mayhorn, Yu Zhang, Harold Kirkham, "Centralized and Decentralized Control for Demand Response," *2011 IEEE PES Innovative Smart Grid Technologies (ISGT)*, pp.1-8.

[4] NERC Technical Document, Balancing and Frequency Control, January 26, 2011: http://www.nerc.com/docs/oc/rs/NERC%20Balancing%20and%20Frequency%20Control%20040520111.pdf

[5] National Energy Technology Laboratory, Frequency Instability Problems in North American Interconnections, Report DOE/NETL-2011/1473, May 1, 2011: http://www.netl.doe.gov/energy-analyses/pubs/TransmissionFreqProb.pdf

[6] FERC. "Order 745: Demand Response Compensation in Organized Wholesale Energy Markets". 2011; Available from: http://www.ferc.gov/EventCalendar/Files/20110315105757-RM10-17-000.pdf.

[7] FERC. "Order 755: Frequency Regulation Compensation in Organized Wholesale Power Markets". 2011; Available from: http://www.ferc.gov/whats-new/commmeet/2011/102011/E-28.pdf.

[8] Jason MacDonald, Peter Cappers, Duncan Callaway, Sila Kiliccote, "Demand Response Providing Ancillary Services : A Comparison of Opportunities and Challenges in the US Wholesale Markets," Grid-Interop Forum 2012, Dec 3-6, Irving, TX, USA http://www.gridwiseac.org/pdfs/forum_papers12/macdonald_paper_gi12.pdf

[9] S. Kiliccote, M.A. Piette, G. Ghatikar, E. Koch, D. Hennage , J. Hernandez, A. Chiu, O. Sezgen, J. Goodin, "Open Automated Demand Response Communications in Demand Response for Wholesale Ancillary Services," Grid-Interop Forum 2009, Denver, CO, November 17-19, http://drrc.lbl.gov/sites/drrc.lbl.gov/files/lbnl-2945e.pdf

[10] FERC. "A National Assessment of Demand Response Potential". 2009 June; Available from: http://www.ferc.gov/legal/staff-reports/06-09-demand-response.pdf

[11] ENTSO-E Network Code on Demand Connection, 21 Dec 2012: https://www.entsoe.eu/fileadmin/user_upload/_library/resources/DCC/ENTSO-E_finalises_DCC/121221_final_Network_Code_on_Demand_Connection.pdf

[12] J.H. Eto, C. Bernier, J. Kueck,J. Nelson-Hoffman, P. Young, B. Kirby, E. Parker, D. Sheehan, "The Demand Response Spinning Reserve Demonstration – Measuring the Speed and Magnitude of Aggregated Demand Response", *2012 45th Hawaii International Conference on System Sciences*, 4-7 Jan. 2012, Maui, USA.

[13] S. Ali Pourmousavi, M. Hashem Nehrir, "Real-Time Central Demand Response for Primary Frequency Regulation in Microgrids," *IEEE Trans. on Smart Grid*, Vol. 3, No. 4, Dec 2012, pp. 1988-1996.

[14] Z. Xu, J. Østergaard, M. Togeby "Demand as Frequency Controlled Reserve", *IEEE Trans. on Power Systems*, Vol. 26, No. 3, August 2011, pp. 1062-1071.

[15] K. Samarakoon, J. Ekanayake, N. Jenkins, "Investigation of Domestic Load Control to Provide Primary Frequency Response Using Smart Meters", *IEEE Trans. on Smart Grid*, Vol. 3, No. 1, March 2012, pp. 282-292.

[16] Joe A. Short, David G. Infield, and Leon L. Freris "Stabilization of Grid Frequency Through Dynamic Demand Control," *IEEE Transactions on Power Systems*, vol. 22, no. 3, pp. 1284-1293, August 2007.

[17] Joseph H. Eto, "Demand Response Spinning Reserve Demonstration," Ernest Orlando Lawrence Berkeley National Laboratory, May 2007 http://certs.lbl.gov/pdf/62761.pdf

[18] A. Molina-García, F. Bouffard, D. S. Kirschen "Decentralized Demand-Side Contribution to Primary Frequency Control," *IEEE Trans. on Power Systems*, Vol. 26, No. 1, February 2011, pp. 411-1071.

[19] JC Fuller, B Vyakaranam, N Prakash Kumar, SM Leistritz, GB Parker, Modeling of GE Appliances in GridLAB-D: Peak Demand Reduction, PNNL-21358, April 2012

[20] J. Kondoh, N. Lu, and D. J. Hammerstrom, "An evaluation of the water heater load potential for providing regulation service," *IEEE Trans.Power Syst.*, vol. 26, no. 3, pp. 1309–1316, 2011.

[21] JC Fuller, GB Parker, Modeling of GE Appliances: Cost Benefit Study of Smart Appliances in Wholesale Energy, Frequency Regulation, and Spinning Reserve Markets, PNNL- 22128, Dec 2012

[22] M Donnelly, S Mattix, D Trudnowski, JE Dagle, Autonomous Demand Response for Primary Frequency Regulation, PNNL- 21152, Jan 2012

[23] Mattix, S.R. ; Donnelly, M.K. ; Trudnowski, D.J. ; Dagle, J.E., "Autonomous Demand Response for Frequency Regulation on a Large-Scale Model of an Interconnected Grid," *2012 IEEE Power and Energy Society General Meeting*, pp.1 – 8.

[24] H. Ni, "PJM Advanced Technology Pilots for System Frequency Control," *2012 IEEE Power and Energy Society General Meeting*, pp.1 – 6.

[25] C. Diduch, M.Shaad, R. Errouissi, M.E.Kaye, J.Meng, L.Chang "Aggregated Domestic Electric Water Heater Control –Building on Smart Grid Infrastructure," *2012 IEEE 7th International Power Electronics and Motion Control Conference –ECCE Asia June 2-5*, Harbin, China, pp.1-8

[26] T.M. Keep, F.E. Sifuentes, D.M. Auslander, D.S. Callaway, "Using load Switches to control aggregated electricity demand for load following and
regulation", 2011 IEEE PES General Meeting, Detroit, USA, pp.1-7.

[27] B. Biegel, L. Henrik Hanse, P. Andersen, J. Stoustrup, "Primary Control by ON/OFF Demand-Side Devices," *IEEE Trans. on Smart Grid*, Early Access July 2013, pp.1-12

[28] EnerNOC, "Demand response: A multi-purpose resource for utilities and grid operators," 2012. http://www.enernoc.com/images/whitepapers/pdfs/drmultipurpose.pdf

[29] P. J. Douglass, R. Garcia-Valle, P. Nyeng, J. Østergaard, and M. Togeby, "Demand as frequency controlled reserve: Implementation and practical demonstration," in *Proc. Innovative Smart Grid Technol.Conf.*, Manchester, U.K., 2011, pp. 1–7.

[30] I Kamwa, R Grondin, D Asber, JP Gingras, G Trudel, "Active-power stabilizers for multimachine power systems: challenges and prospects," *IEEE Transactions on Power Systems*, **13** (4), 1352-1358

[31] I Kamwa, R Grondin, D Asber, JP Gingras, G Trudel Large-scale active-load modulation for angle stability improvement", *IEEE Transactions on Power Systems*, **14** (2), 582-590

[32] B. Ramanathan, V. Vittal, "Small–Disturbance Angle Stability Enhancement Through Direct Load Control, Parts I & II" *IEEE Transactions on Power Systems*, **21** (2), May 2006, pp.773-790

[33] "A national assessment of demand response potential," Federal Energy Regulatory Commission, Jun. 2009 [Online]. Available: http://www.ferc.gov/legal/staff-reports/06-09-demand-response.pdf,

[34] Z. Xu, J. Østergaard, and M. Togeby, Demand as Frequency Controlled Reserve—*Final Report of the PSO Project, Technical University of Denmark and Ea Energy Analyses, 2008.*

[35] Z. Xu, J. Østergaard, M. Togeby, and C. Marcus-Møller, "Design and modeling of thermostatically controlled loads as frequency controlled reserve," *in Proc. 2007 IEEE PES General Meeting.*

[36] Hammerstrom DJ, R Ambrosio, TA Carlon, JG DeSteese, GR Horst, R Kajfasz, LL Kiesling, P Michie, RG Pratt, M Yao, J Brous, DP Chassin, RT Guttromson, OM Jarvegren, S Katipamula, NT Le, TV Oliver, and SE Thompson, "Pacific Northwest GridWise Testbed Demonstration Projects; Part I. Olympic Peninsula Project", PNNL-17167, 2008, Pacific Northwest National Laboratory, Richland, WA.

[37] Hammerstrom DJ, J Brous, DP Chassin, GR Horst, R Kajfasz, P Michie, TV Oliver, TA Carlon, C Eustis, OM Jarvegren, W Marek, RL Munson, and RG Pratt, "Pacific Northwest GridWise Testbed Demonstration Projects; Part II. Grid FriendlyAppliance Project," PNNL-17079, 2007, Pacific Northwest National Laboratory, Richland, WA.

[38] D. Trudnowski, M. Donnelly and E. Lighter, "Power-System Frequency and Stability Control using Decentralized Intelligent Loads", IEEE PES Transmission and Distribution Conference and Exhibition, 2005/2006, May 2006, Dallas, TX.

[39] IEEE recommended practice for excitation system models for power system stability studies: IEEE St.421.5-2002(Section 9)

[40] Ruisheng Diao ; Shuai Lu ; Elizondo, M. ; Mayhorn, E. ; Yu Zhang ; Samaan, "Electric water heater modeling and control strategies for demand response," *Power and Energy Society General Meeting, IEEE,* 2012 , pp: 1 – 8

[41] http://www.mathworks.com/help/physmod/sps/powersys/ref/threephasedynamicload.html

[42] P.K. Dash, M. Padhee, S.K. Barik, "Estimation of power quality indices in distributed generation systems during power islanding conditions," *Elect. Power and Energy Syst.*, 36 (2012), pp.18–30